Breakdown of nonlinear elasticity in amorphous solids at finite temperatures

Itamar Procaccia,* Corrado Rainone, Carmel A. B. Z. Shor, and Murari Singh
Department of Chemical Physics, The Weizmann Institute of Science, Rehovot 76100, Israel
(Received 16 March 2016; published 13 June 2016)

It is known [H. G. E. Hentschel *et al.*, Phys. Rev. E **83**, 061101 (2011)] that amorphous solids at zero temperature do not possess a nonlinear elasticity theory: besides the shear modulus, which exists, none of the higher order coefficients exist in the thermodynamic limit. Here we show that the same phenomenon persists up to temperatures comparable to that of the glass transition. The zero-temperature mechanism due to the prevalence of dangerous plastic modes of the Hessian matrix is replaced by anomalous stress fluctuations that lead to the divergence of the variances of the higher order elastic coefficients. The conclusion is that in amorphous solids elasticity can never be decoupled from plasticity: the nonlinear response is very substantially plastic.

DOI: 10.1103/PhysRevE.93.063003

I. INTRODUCTION

By cooling glass-forming liquids below their glass transition temperature one forms amorphous solids. They are solid because particles are not free to move ergodically but, rather, can only vibrate around equilibrium positions. They are amorphous because, differently from crystals, these positions possess no long-range periodicity. As a result, a glass sample is always unique: while the structure of a crystalline solid is always realized in the same manner (barring local defects), the amorphous structure of a glass is randomly selected [1,2]. So, even if an ensemble of glasses is prepared with a perfectly reproducible protocol, one always ends up with pieces of material with different structural properties. Is it important to know whether these structural differences have any important effect on the physical observables of the glass, or, in other words, which observables would *self-average* such that their sample-to-sample fluctuations would be negligible in the thermodynamic limit. Self-averaging assumptions go a long way back, at least to Tool's first work on fictive temperatures [3], and are a basic underlying assumption in the field of study of the thermodynamics of disordered systems in general [4], beyond structural glasses. As a matter of fact, self-averaging can be shown to be rigorously realized (at least for systems with short-range interactions) for extensive quantities as a consequence of the central limit theorem [4]. From an experimental point of view, this means that if one measured an extensive observable (say, the internal energy or the thermal capacity) in a given glass, the result would be representative of all the glasses manufactured with the same protocol. From a theoretical point of view, this means that some properties of glassy states can be safely computed by averaging them over the amorphous structures available [5,6]. The assumption of self-averaging is not sufficiently scrutinized for intensive variables. While some observables strictly related to the structure of the glass, such as the refractive index [7], do not self-average, it is still a common assumption that all thermodynamic quantities, whether extensive or intensive, should share this property.

In this paper we show that this expectation is *not* met in the case of the nonlinear elastic coefficients [8] of a model molecular glass at *any temperature* below the glass transition. This leads to a breakdown of the elastic theory for the material. It has been shown that this is the case for amorphous solids at zero temperature [9]; however, one could think that temperature fluctuations might destroy the relevance of the findings at $T = 0$. We show in this paper that this is not so: the presence of anomalous sample-to-sample fluctuations of nonlinear elastic coefficients leads to a breakdown of elasticity theory also in amorphous solids at experimentally and practically relevant temperatures.

II. EXPRESSIONS OF ELASTIC COEFFICIENTS

Let us consider a standard elasticity theory for a solid under simple shear strain (with $\gamma_{xy} = \gamma$ the only nonzero component of the strain tensor). This is written in the form of a Taylor expansion around zero strain [8],

$$\sigma(\gamma) = B_1\gamma + \frac{1}{2!}B_2\gamma^2 + \frac{1}{3!}B_3\gamma^3 + \cdots , \tag{1}$$

where $\sigma = \sigma_{xy}$ is the only nonzero component of the stress tensor and

$$B_n \equiv \left.\frac{d^n\sigma}{d\gamma^n}\right|_{\gamma=0} . \tag{2}$$

B_1 is the usual shear modulus, which is usually denoted μ, with $\mu \equiv B_1$. In a thermal setting, the stress can be written as a canonical ensemble average [10–12],

$$\sigma(\gamma) \equiv \frac{1}{V}\left\langle\frac{dU}{d\gamma}\right\rangle = \frac{1}{V}\frac{1}{Z(\gamma)}\int_{X\in\alpha(R)} dX\,\frac{dU}{d\gamma}e^{-\beta U_\gamma(X)}, \tag{3}$$

where, as usual, $\beta \equiv \frac{1}{k_BT}$ and V is the system's volume, $U(X)$ is the system's potential energy, and the strain is implemented through an affine transformation of particle coordinates [10]. The canonical average is replaced below by a time average, using time intervals τ for which the variables measured reach a stationary value, but with τ being much shorter than the glass relaxation time (usually denoted τ_α). This time interval allows the system to visit a *restricted* domain $\alpha(R)$ of configurations; accordingly, the integral is computed over this set of configurations, which are visited by the glass particles that are confined around an amorphous structure R [5,13].

*itamar.procaccia@weizmann.ac.il

To compute the elastic coefficients, one needs only to take derivatives of Eq. (3) with respect to the strain. Note how in Eq. (3) the strain parameter is contained in the derivative $\frac{dU}{d\gamma}$, in the Boltzmann factor, and in the partition function $Z(\gamma)$. When taking further derivatives of the derivative term, one will, in general, get a term of the kind $\langle \frac{\partial^n U}{\partial \gamma^n} \rangle$, while derivatives of the partition function and Boltzmann factor will yield cumulants of the stress and additional covariance terms. The shear modulus, for example, has the expression [13]

$$\mu \equiv B_1 = \frac{1}{V}\left\langle \frac{\partial^2 U}{\partial \gamma^2} \right\rangle - \beta V[\langle \sigma^2 \rangle - \langle \sigma \rangle^2], \tag{4}$$

which is the sum of a generalization of the *Born term* found in crystalline solids [14] and thermal fluctuations of the stress. For the first nonlinear coefficient B_2 one has

$$B_2 = \frac{1}{V}\left\langle \frac{\partial^3 U}{\partial \gamma^3} \right\rangle - 3\beta V[\langle \sigma' \sigma \rangle - \langle \sigma' \rangle \langle \sigma \rangle] + (\beta V)^2 \langle (\sigma - \langle \sigma \rangle)^3 \rangle, \tag{5}$$

where we have used the compact notation $\sigma' = \frac{\partial \sigma}{\partial \gamma}$. In Appendix A we derive the expressions for the nonlinear coefficients up to third order. Since these coefficients are computed by sampling a glassy space of configurations selected by an amorphous structure, their values will depend on the particular glass sample under consideration, as detailed in Sec. I. We are interested in their probability distribution over samples and, in particular, in sample-to-sample fluctuations,

$$\overline{(\delta B_n)^2} \equiv \overline{(B_n - \overline{B_n})^2}, \tag{6}$$

where $\overline{(\cdot)}$ denotes the average over samples. Naive central limit theorem considerations suggest that $\overline{(\delta B_n)^2} \simeq \frac{1}{V}$, which would imply self-averaging. In the following we present evidence that this assumption fails for all $n \geqslant 2$.

III. NUMERICAL SIMULATIONS

A. Method

We compute the elastic coefficients B_n up to third order from molecular dynamics (MD) simulations of a Kob-Andersen [15] 65/35 binary mixture in two dimensions. The Lennard-Jones (LJ) potentials used are presented in Appendix B together with the details of the simulations. We always start by simulating the liquid at $T = 0.4$, whereupon the relaxation of the binary correlation function is still exponential. Next we cool the system at a rate of 10^{-6} in LJ time units, as explained in Appendix B, to the final target temperature of $T = 10^{-6}$. The system is now heated up instantaneously to a working temperature in the range $T \in [0.05, 0.25]$ in steps of 0.05. The system is then "equilibrated" by running 100 000 MD steps. To measure any desired quantity we now run $\tau = 200\,000$ MD steps and measure the time average of the said quantity. Thus, for example, if we want to measure $\langle \sigma^4 \rangle$ we compute

$$\langle \sigma^4 \rangle \equiv \tau^{-1} \sum_{i=1}^{\tau} \sigma^4(t_i), \tag{7}$$

where t_i are the MD steps. Having computed the desired quantity in this way, we repeat the process 1000 times, using different initial configurations from the run at $T = 0.4$, each of which will yield a different glass sample, or realization. The values found are histogrammed and normalized to yield a probability distribution function (pdf). This pdf is then used to evaluate the average over the 1000 samples and the variance, Eq. (6). Our numerical setup is thus equivalent to the production of an ensemble of glass samples, each manufactured with the same, exactly reproduced protocol.

B. Results

A representative set of results for the distributions of B_1, B_2, and B_3 over the realizations is shown in Fig. 1 for $T = 0.15$. Similar results are seen for the entire temperature range: the distribution of the shear modulus over the realizations sharpens with the system size, indicating self-averaging in the thermodynamic limit. The distributions of B_2 and B_3 (and, in fact, of all B_n with $n \geqslant 2$) broaden rapidly with increasing system size, indicating a breakdown of self-averaging and of nonlinear elasticity. The rate of broadening of the distributions increases with the order of the coefficient under consideration. As an example, let us consider the variances of the distributions of the first three moduli; to evaluate their finite-size scaling, we perform Gaussian least-squares fits of the data and consider the resulting variances, which are shown in Fig. 2 as a function of the system size at different temperatures. One should stress that measuring the variances without Gaussian fits is a bit noisier but it yields very similar scaling plots as a function of the system size.

Denoting the variance of B_k as $\overline{(\delta B_k)^2}$ we find that

$$\overline{(\delta B_1)^2} \sim N^{\alpha_1}, \quad \overline{(\delta B_2)^2} \sim N^{\alpha_2}, \quad \overline{(\delta B_3)^2} \sim N^{\alpha_3}, \tag{8}$$

with $\alpha_1 = -0.68 \pm 0.08$, $\alpha_2 = 0.78 \pm 0.05$, and $\alpha_3 = 1.92 \pm 0.06$ independently of the temperature in the range $T \in [0.05, 0.25]$.

To shed light on the breakdown of self-averaging it is useful to consider the sample-to-sample fluctuations of the moments of the stress. We note that fluctuations in the Born-like terms in any of the B_k moduli are always convergent. The reason for divergence are the moments $\langle \sigma^k \rangle$ which appear in the expressions for the coefficients B_k, multiplied by a suitable factor of $V^{k-1} \sim N^{k-1}$ to make all the B_k's intensive. It is therefore interesting to consider the sample-to-sample fluctuations of $X_k \equiv N^{k-1}\langle \sigma^k \rangle$. Accordingly, we consider the pdf's of $P(X_k)$ over our glass samples. In Fig. 3 we show representative results of these pdf's in a rescaled form. The upshot of the analysis is that we can collapse the data for these pdf's for different system sizes if we plot $N^{k/2-1}P(X_k)$ as a function of $N^{k/2}\langle \sigma^k \rangle$. It is an immediate exercise therefore to evaluate the system-size dependence of the variance of X_k, denoted here $\overline{(\delta \mathbf{X}_k)^2}$, obtaining the scaling dependence,

$$\overline{(\delta \mathbf{X}_k)^2} \sim N^{k-2}, \tag{9}$$

independently of the temperature. It now becomes clear that the convergent result for $\overline{(\delta B_1)^2}$ and the fact that $\alpha_2 < 1$ and $\alpha_3 < 2$ must follow from a cancellation of the leading N

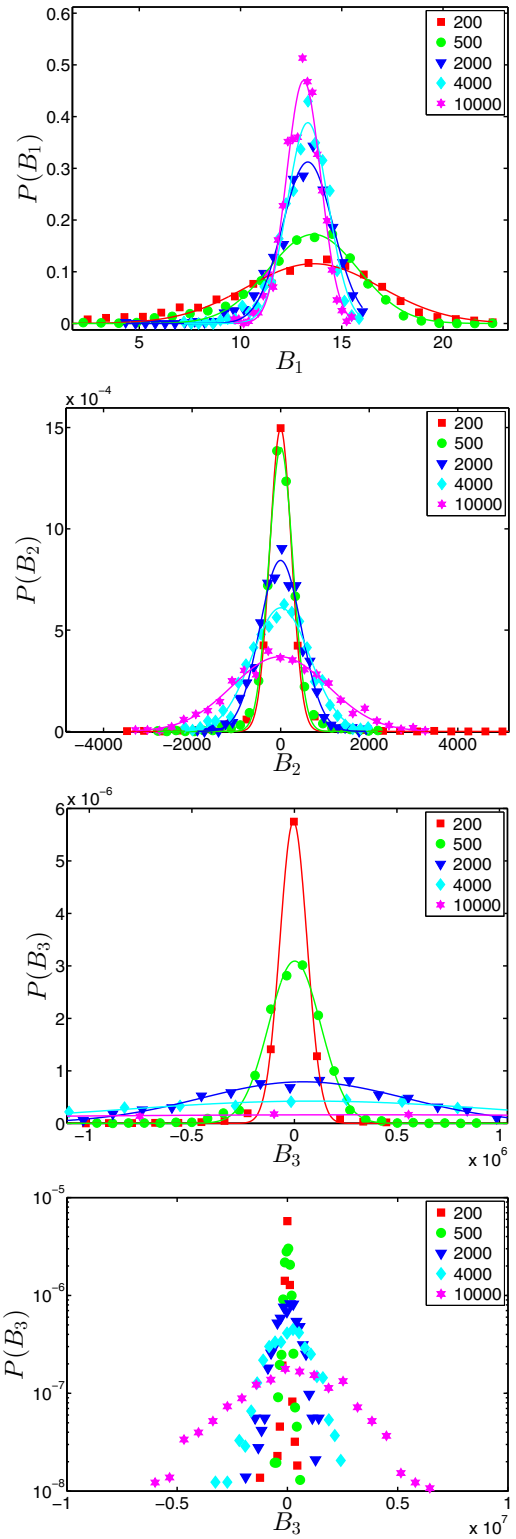

FIG. 1. Distributions of $B_1 = \mu$, B_2, and B_3 over the realizations for $T = 0.15$, for system sizes from $N = 200$ to $N = 10\,000$. Lines are Gaussian fits to the data, from which we compute the variances. The distribution of the shear modulus sharpens when the system size increases. The distributions of B_2 and B_3 broaden with increasing system size, refuting any hope for self-averaging. The distributions of higher order coefficients broaden more and more rapidly. In the last panel we present the same data for B_3 semilogarithmically, to stress the complete form of the pdf of B_3.

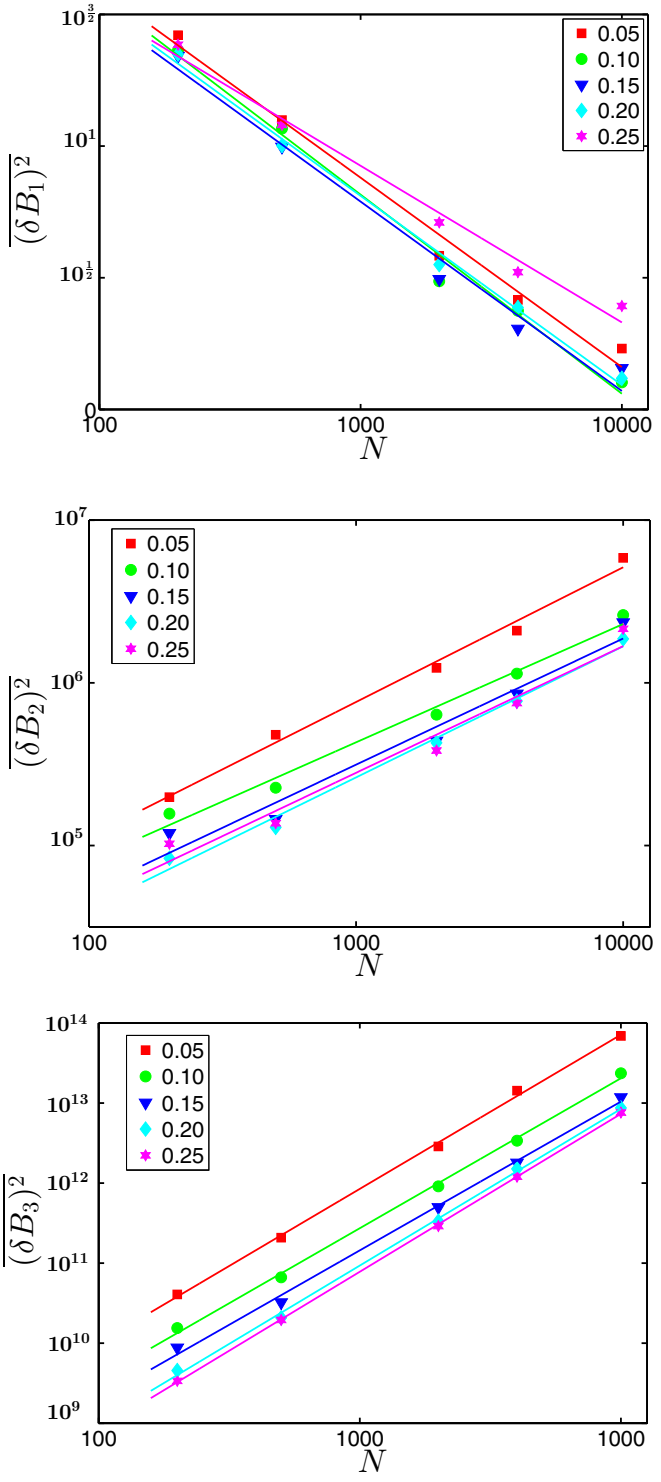

FIG. 2. Variances of B_1, B_2, and B_3 over the realizations as a function of the system size for different temperatures. Lines are least-square fits to the data. Note that, to within the available accuracy, the system-size dependence of the variances appears to be temperature independent, at least up to $T = 0.25$.

dependence in the terms involving stress fluctuations. A precise determination of the scaling exponents and the question of their universality or nonuniversality must await a very extensive set of numerical

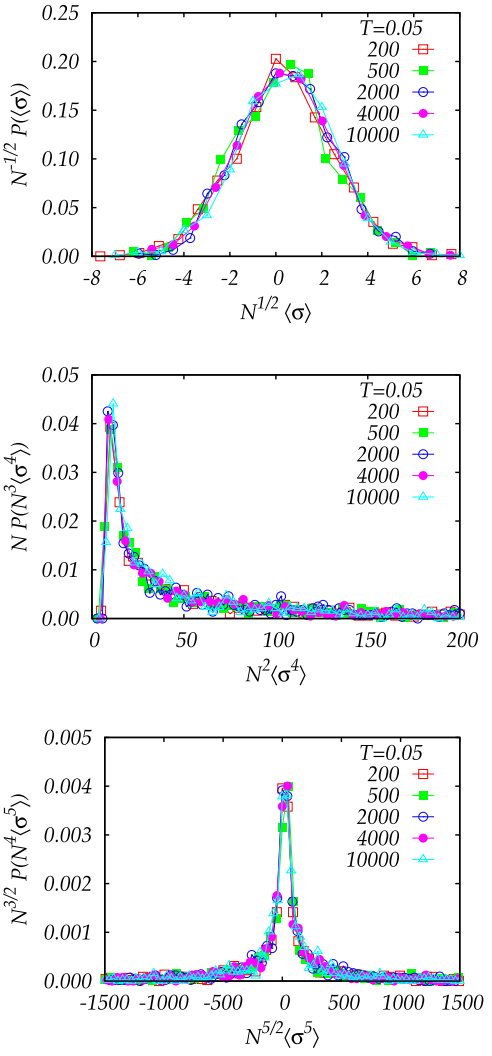

FIG. 3. Examples of rescaled pdf's of X_k for $k = 1$, 4, and 5, multiplied by $N^{k/2-1}$ and plotted as a function of $N^{k/2}\langle\sigma^k\rangle$ at $T = 0.05$. Similar data collapses are found for other k values and for other temperatures without changing the exponents. A similar data collapse for $k = 2$, 3, and 6 can be found in Appendix B.

simulations which are outside the scope of this paper.

IV. DISCUSSION

It is interesting to examine the correspondence between the divergence of the variances of the nonlinear elastic coefficients at $T = 0$ and that at a finite temperature. At $T = 0$ the expression for the shear modulus, instead of Eq. (4), reads [16]

$$B_1(T=0) = \frac{1}{V}\frac{\partial^2 U}{\partial\gamma^2} - \frac{1}{V}\boldsymbol{\Xi}\cdot\boldsymbol{H}^{-1}\cdot\boldsymbol{\Xi}, \qquad (10)$$

where $\boldsymbol{H}$ is the Hessian matrix and $\boldsymbol{\Xi} \equiv \partial^2 U/\partial \boldsymbol{r}_i\partial\gamma$. Higher order nonlinear moduli contain three, five, and more factors of $\boldsymbol{H}^{-1}$ and their sample-to-sample fluctuations stem from the existence of arbitrarily small eigenvalues of the Hessian matrix when the system size increases [9]. It can be proven that the stress fluctuation term in Eq. (4) approaches smoothly the second term in Eq. (10) and that the cumulant terms in $B_k(T)$ approach in the same way the analogous term of the athermal counterpart (see [17] and Appendix C). In recent years, much research has been devoted to the concept of *marginality* [18] in disordered systems, which can be broadly defined as the possibility of destabilizing a system with a generic perturbation without having to pay an energy cost. In the case of athermal systems, such as jammed packings, these perturbations are *mechanical* in nature (for example, the opening of a contact between two grains in a packing) and marginality manifests under the guise of arbitrarily low-lying eigenvalues in the Hessian of the system, related to floppy modes that can be excited with no energy cost. As detailed in [9], these are precisely the modes that cause the breakdown of nonlinear elasticity in athermal glasses. The correspondence between the second term in Eq. (10) and the stress fluctuations in the thermal case (which, as we pointed out, cause the breakdown of nonlinear elasticity in the present case) highlights how the mechanical marginality found in athermal amorphous systems must have a thermal, thermodynamic counterpart in terms of the presence of anomalous thermal fluctuations, which in turn induce, through the fluctuation-dissipation theorem, an anomalous response of the system to even arbitrarily small thermodynamic perturbations, such as strain or a magnetic field. We argue that a better understanding of the links between mechanical and thermal marginality is paramount for the final achievement of a complete and consistent theoretical picture of the physics of amorphous systems.

Finally, we should relate these findings to a recent theoretical work [19] predicting a so-called Gardner transition [20] in thermal glass-forming liquids [19,21]. Fundamentally the prediction is that at some temperature, lower than the glass transition temperature, there should be a qualitative change in the nature of the free-energy landscape, generating a rough scenery with arbitrarily small barriers between local minima. The connection to the present work is that this phenomenon is accompanied by a breakdown of nonlinear elasticity in much the same way as reported above. The available theory pertains to a mean-field treatment, and comparison of exponents is probably not warranted. Nevertheless, it is interesting that the shear modulus is expected to exist, and the variances of B_k with $k \geqslant 3$ are expected to diverge with the system size, in agreement with the predictions in Ref. [9] and the findings in the present paper. In Ref. [19] it is also predicted that the phenomenon should disappear when the system is heated above the (protocol-dependent) Gardner temperature, a claim that we are not in a position to confirm or refute. A careful search for a putative Gardner temperature would require repeating our analysis on extremely slowly quenched glasses as a way to provide a good separation of the Gardner point and the point of disappearance of the shear modulus [19]. Such an analysis is beyond the scope of the present paper but appears to be a worthwhile endeavor for future research.

ACKNOWLEDGMENTS

The authors benefited from useful discussions with Giulio Biroli and Pierfrancesco Urbani. This work was supported in

part by the ERC "ideas" grant STANPAS and by the Minerva Foundation, Munich Germany.

APPENDIX A: EXPRESSIONS OF THE ELASTIC COEFFICIENTS

We present here the expressions of the elastic coefficients that are studied in the text. We start from the definition of the stress,

$$\sigma = \frac{1}{V}\left[\frac{1}{Z(\gamma)}\int \frac{dU}{d\gamma}e^{-\beta U(\gamma)}dX\right], \tag{A1}$$

where

$$Z(\gamma) = \int e^{-\beta U(\gamma)}dX. \tag{A2}$$

We now take a derivative of this expression with respect to γ, which by definition will be equal (once computed at $\gamma = 0$) to the shear modulus. We get

$$\frac{d\sigma}{d\gamma} = \frac{1}{V}\left[\frac{1}{Z(\gamma)}\int \frac{\partial^2 U}{\partial\gamma^2}e^{-\beta U(\gamma)}dX - \beta\frac{1}{Z(\gamma)}\int\left(\frac{\partial U}{\partial\gamma}\right)^2 \times e^{-\beta U(\gamma)}dX + \beta\frac{1}{Z(\gamma)^2}\left(\int \frac{\partial U}{\partial\gamma}e^{-\beta U(\gamma)}dX\right)^2\right],$$

since

$$\frac{\partial}{\partial\gamma}Z(\gamma) = -\beta\int \frac{\partial U}{\partial\gamma}e^{-\beta U(\gamma)}dX; \tag{A3}$$

now, since σ is an intensive quantity, $\sigma \equiv \frac{1}{V}\langle\frac{\partial U}{\partial\gamma}\rangle$, we have to multiply the last two terms by $\frac{V}{V}$, and we, finally, get

$$\mu = \frac{1}{V}\left\langle\frac{\partial^2 U}{\partial\gamma^2}\right\rangle - \beta V[\langle\sigma^2\rangle - \langle\sigma\rangle^2], \tag{A4}$$

as reported in the text and in [13]. We now take further derivatives in order to compute the second- and third-order coefficients. For the second derivative we have

$$\begin{aligned}\frac{d^2\sigma}{d\gamma^2} = \frac{1}{V}\Bigg[&\frac{1}{Z}\int\frac{\partial^3 U}{\partial^3\gamma}e^{-\beta U}dX + \beta\frac{1}{Z^2}\int\frac{\partial^2 U}{\partial\gamma^2}e^{-\beta U}dX\int\frac{\partial U}{\partial\gamma}e^{-\beta U}dX - 3\beta\frac{1}{Z}\int\frac{\partial U}{\partial\gamma}\frac{\partial^2 U}{\partial\gamma^2}e^{-\beta U}dX\\ &- \beta^2\frac{1}{Z^2}\int\frac{\partial U}{\partial\gamma}e^{-\beta U}dX\int\frac{\partial^2 U}{\partial\gamma^2}e^{-\beta U}dX + \beta^2\frac{1}{Z}\int\left(\frac{\partial U}{\partial\gamma}\right)^3 e^{-\beta U}dX\\ &+ 2\beta\left(\frac{1}{Z}\int\frac{\partial U}{\partial\gamma}e^{-\beta U}dX\right)\left(\frac{1}{Z}\int\frac{\partial^2 U}{\partial\gamma^2}e^{-\beta U}dX - \frac{\beta}{Z(\gamma)}\int\left(\frac{\partial U}{\partial\gamma}\right)^2 e^{-\beta U}dX + \frac{\beta^2}{Z(\gamma)^2}\left(\int\frac{\partial U}{\partial\gamma}e^{-\beta U}dX\right)^2\right)\Bigg];\end{aligned}$$

and once we have taken care of the volume factors, we get the final result for B_2,

$$\begin{aligned}B_2 &= \frac{1}{V}\left\langle\frac{\partial^3 U}{\partial\gamma^3}\right\rangle - 3\beta V[\langle\sigma'\sigma\rangle - \langle\sigma'\rangle\langle\sigma\rangle] + (\beta V)^2\langle(\sigma - \langle\sigma\rangle)^3\rangle\\ &= \frac{1}{V}\left\langle\frac{\partial^3 U}{\partial\gamma^3}\right\rangle - 3\beta V\mathrm{Cov}[\sigma',\sigma] + (\beta V)^2\kappa_3[\sigma],\end{aligned} \tag{A5}$$

as reported in the text. Higher order coefficients can be computed with the same method, and even though the expressions become longer and cumbersome, the calculation in itself is trivial. The result for B_3, for example, is

$$\begin{aligned}B_3 =& \frac{1}{V}\left\langle\frac{\partial^4 U}{\partial\gamma^4}\right\rangle + 3\beta V\langle\sigma'\rangle^2 - 3\beta V\langle(\sigma')^2\rangle + 4\beta V\langle\sigma''\rangle\langle\sigma\rangle - 4\beta V\langle\sigma''\sigma\rangle + 6\beta^2V^2\langle\sigma^2\sigma'\rangle - 6\beta^2V^2\langle\sigma^2\rangle\langle\sigma'\rangle\\ &+ 12\beta^2V^2\langle\sigma\rangle^2\langle\sigma'\rangle - 12\beta^2V^2\langle\sigma\rangle\langle\sigma\sigma'\rangle + \beta^3V^3(4\langle\sigma^3\rangle\langle\sigma\rangle + 3\langle\sigma^2\rangle^2 - 12\langle\sigma^2\rangle\langle\sigma\rangle^2 + 6\langle\sigma\rangle^4 - \langle\sigma^4\rangle)\\ =& \frac{1}{V}\left\langle\frac{\partial^4 U}{\partial\gamma^4}\right\rangle - 3\beta V[\langle(\sigma')^2\rangle - \langle\sigma'\rangle^2] - 4V\beta[\langle\sigma''\sigma\rangle - \langle\sigma''\rangle\langle\sigma\rangle] + 6V^2\beta^2[\langle\sigma'\sigma^2\rangle - \langle\sigma'\rangle\langle\sigma^2\rangle]\\ &- 12V^2\beta^2\langle\sigma\rangle[\langle\sigma\sigma'\rangle - \langle\sigma\rangle\langle\sigma'\rangle] + 3V^3\beta^3(\langle\sigma^2\rangle - \langle\sigma\rangle^2)^2 - V^3\beta^3\langle(\sigma - \langle\sigma\rangle)^4\rangle\\ =& \frac{1}{V}\left\langle\frac{\partial^4 U}{\partial\gamma^4}\right\rangle - 3V\beta\mathrm{Var}[\sigma'] - 4V\beta\mathrm{Cov}[\sigma'',\sigma] + 6V^2\beta^2\mathrm{Cov}[\sigma',\sigma^2]\\ &- 12V^2\beta^2\mathrm{E}[\sigma]\mathrm{Cov}[\sigma,\sigma'] + 3V^3\beta^3(\mathrm{Var}[\sigma])^2 - V^3\beta^3\kappa^4[\sigma].\end{aligned}$$

APPENDIX B: DETAILS ON THE NUMERICS

1. Model details

We study the two-dimensional Kob-Andersen binary mixture with a 65:35 ratio of particles A and B, where particles are point particles and interact via shifted and smoothed Lennard-Jones potentials, $u_{\alpha\beta}(r)$, given by

$$u_{\alpha\beta}(r) = \begin{cases} u^{\mathrm{LJ}}_{\alpha\beta} + A_{\alpha\beta} + B_{\alpha\beta}r + C_{\alpha\beta}r^2 & \text{if} \quad r \leqslant R^{\mathrm{cut}}_{\alpha\beta},\\ 0 & \text{if} \quad r > R^{\mathrm{cut}}_{\alpha\beta},\end{cases} \tag{B1}$$

where

$$u_{\alpha\beta}^{\rm LJ} = 4\epsilon_{\alpha\beta}\left[\left(\frac{\sigma_{\alpha\beta}}{r}\right)^{12} - \left(\frac{\sigma_{\alpha\beta}}{r}\right)^{6}\right]. \tag{B2}$$

The smoothing of the potentials in Eq. (B1) is such that they vanish with two zero derivatives at distances $R_{\alpha\beta}^{\rm cut} = 2.5\sigma_{\alpha\beta}$. The parameters for smoothing the LJ potentials in Eq. (B1) and for A- and B-particle-type interactions in Eq. (B2) [15] are given in the following table:

Interaction	$\sigma_{\alpha\beta}$	$\epsilon_{\alpha\beta}$	$A_{\alpha\beta}$	$B_{\alpha\beta}$	$C_{\alpha\beta}$
AA	1.00	1.0	0.4527	−0.3100	0.0542
BB	0.88	0.5	0.2263	−0.1762	0.0350
AB	0.80	1.5	0.6790	−0.5814	0.1271

The reduced units for mass, length, energy, and time have been taken as m, σ_{AA}, ϵ_{AA}, and $\sigma_{AA}\sqrt{m/\epsilon_{AA}}$, respectively.

2. Simulation details

All simulations were carried out with MD under *NVT* conditions, using a velocity-Verlet algorithm with a time step of $\Delta t = 0.005$ in reduced units. A Berendsen thermostat, with a time constant of 5 in reduced units, was used to maintain the desired temperature. All simulations were performed at a constant density $\rho = 1.162$, with system sizes ranging from $N = 200$ to $N = 10\,000$ and a temperature range from $T = 0.05$ to $T = 0.25$, with a gap of 0.05. At the highest temperature, $T = 0.25$, the averaging time needed to stabilize the moments of the stress is 1000 LJ units, which is orders of magnitude shorter than the τ_α relaxation time at this temperature, which is expected to be about $10^{13} - 10^{15}$ LJ units [22].

3. Protocol for preparation of amorphous solids

In order to prepare amorphous solids, we always start with a random configuration generated at $\rho = 1.162$ and then equilibrate it at a high temperature, $T = 0.4$, for 400 000 MD steps. At this temperature correlation functions still decay exponentially and the system behaves like a liquid. Next, we cool down the system, at a cooling rate of $\Delta T = 10^{-6}$ in reduced units, to a target temperature of $T = 0.000\,001$. We repeat this process starting from different initial conditions at $T = 0.4$ to generate the ensemble of 1000 amorphous solids at each system size.

4. Data collapse for higher order moments

To complement the data presented in Fig. 3 in the text we report in Fig. 4 the data collapse obtained with the scaling ansatz $N^{k/2-1}P(X_k) = f(N^{k/2}\langle\sigma^k\rangle)$ for $k = 2, 3, 6$.

APPENDIX C: LOW-TEMPERATURE LIMIT OF THERMAL FLUCTUATIONS

We show here that, for two generic observables, $A(X)$ and $B(X)$, one has

$$\lim_{\beta\to\infty} \beta[\langle A(X)B(X)\rangle - \langle A(X)\rangle\langle B(X)\rangle] = [\nabla A \cdot \boldsymbol{H}^{-1} \cdot \nabla B]|_{X=X^*}, \tag{C1}$$

where $\boldsymbol{H}^{-1}$ is the inverse Hessian of the system and X^* is the inherent structure into which the system settles when $T \to 0$. The proof is provided in [23] for the case of elastic coefficients; here we report a simpler derivation for two generic

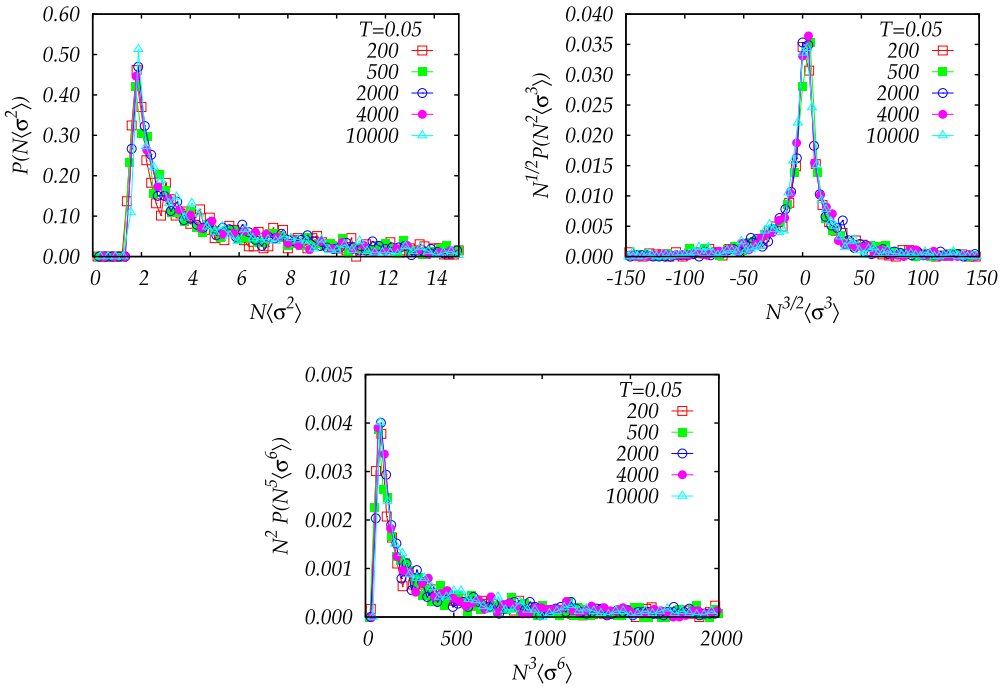

FIG. 4. Data collapse of the $P(X_k)$ obtained with the scaling ansatz reported in the text. Even though it is a purely phenomenological ansatz without a theoretical justification, the results are satisfying.

observables. We start by considering the average,

$$\langle A\rangle = \frac{\int dX\ A(X)e^{-\beta U(X)}}{\int dX\ e^{-\beta U(X)}} = \frac{\int dX\ e^{-\beta[U(X)-\frac{1}{\beta}\log A(x)]}}{\int dX\ e^{-\beta U(X)}}. \quad \text{(C2)}$$

We compute the integrals using the saddle-point method [24]. Let us expand the arguments of the exponentials around the inherent structure. We get, for the numerator,

$$\int dX\ A(X^*)\exp\{-\beta[U(X^*) - \frac{1}{\beta}\frac{1}{B}\nabla B\cdot\delta\mathbf{X} + \frac{1}{2}\delta\mathbf{X}\cdot\boldsymbol{\mathcal{A}}\cdot\delta\mathbf{X} + O(X^3)]\} \quad \text{(C3)}$$

and, for the denominator,

$$\int dX\ \exp\{-\beta[U(X^*) + \frac{1}{2}\delta\mathbf{X}\cdot\boldsymbol{H}\cdot\delta\mathbf{X} + O(X^3)]\}, \quad \text{(C4)}$$

where $\boldsymbol{\mathcal{A}}$ is a matrix defined as

$$\boldsymbol{\mathcal{A}} \to \mathcal{A}_{i\alpha j\beta} \equiv H_{i\alpha j\beta} - \frac{1}{\beta}\frac{\partial^2 \log A}{\partial x_{i\alpha}\partial x_{j\beta}}, \quad \text{(C5)}$$

where the Latin indices denote particle coordinates and the Greek indices spatial axes. The integral in the numerator is a Gaussian integral with a linear term, which can be straightforwardly computed. One gets

$$A(X^*)\exp\left[\frac{1}{2\beta}\left(\frac{\nabla A}{A}\cdot\boldsymbol{\mathcal{A}}^{-1}\cdot\frac{\nabla A}{A}\right)\right]\sqrt{\frac{\pi}{\beta}}^{dN}\frac{1}{\sqrt{\det\boldsymbol{\mathcal{A}}}}, \quad \text{(C6)}$$

while the result for the denominator is

$$\sqrt{\frac{\pi}{\beta}}^{dN}\frac{1}{\sqrt{\det\boldsymbol{H}}}, \quad \text{(C7)}$$

where d is the number of dimensions ($d = 2$ in the present case, but the derivation is valid for any d). In summary, we get, for $\langle A\rangle$,

$$\langle A\rangle \simeq A(X^*)\exp\left[\frac{1}{2\beta}\left(\frac{\nabla A}{A}\cdot\boldsymbol{\mathcal{A}}^{-1}\cdot\frac{\nabla A}{A}\right)\right]\sqrt{\frac{\det\boldsymbol{H}}{\det\boldsymbol{\mathcal{A}}}}, \quad \text{(C8)}$$

so in the $T\to 0$ limit we get, as expected,

$$\lim_{T\to 0}\langle A\rangle = A(X^*). \quad \text{(C9)}$$

Let us now consider $\langle AB\rangle$ and $\langle A\rangle\langle B\rangle$. We get, using the same reasoning,

$$\beta\langle AB\rangle \simeq \beta A(X^*)B(X^*)\exp\left[\frac{1}{2\beta}\left(\frac{\nabla A}{A}+\frac{\nabla B}{B}\right)\cdot\boldsymbol{\mathcal{C}}^{-1}\cdot\left(\frac{\nabla A}{A}+\frac{\nabla B}{B}\right)\right]\sqrt{\frac{\det\boldsymbol{H}}{\det\boldsymbol{\mathcal{C}}}}, \quad \text{(C10)}$$

with the definition

$$\boldsymbol{\mathcal{C}} \to \mathcal{C}_{i\alpha j\beta} \equiv H_{i\alpha j\beta} - \frac{1}{\beta}\frac{\partial^2\log A}{\partial x_{i\alpha}\partial x_{j\beta}} - \frac{1}{\beta}\frac{\partial^2\log B}{\partial x_{i\alpha}\partial x_{j\beta}}, \quad \text{(C11)}$$

while for the other term we get

$$\beta\langle A\rangle\langle B\rangle \simeq \beta A(X^*)B(X^*)\exp\left[\frac{1}{2\beta}\left(\frac{\nabla A}{A}\cdot\boldsymbol{\mathcal{A}}^{-1}\cdot\frac{\nabla A}{A}\right) + \frac{1}{2\beta}\left(\frac{\nabla B}{B}\cdot\boldsymbol{\mathcal{B}}^{-1}\cdot\frac{\nabla B}{B}\right)\right]\sqrt{\frac{\det\boldsymbol{H}}{\det\boldsymbol{\mathcal{A}}}}\sqrt{\frac{\det\boldsymbol{H}}{\det\boldsymbol{\mathcal{B}}}}, \quad \text{(C12)}$$

with the definition

$$\boldsymbol{\mathcal{B}} \to \mathcal{B}_{i\alpha j\beta} \equiv H_{i\alpha j\beta} - \frac{1}{\beta}\frac{\partial^2\log B}{\partial x_{i\alpha}\partial x_{j\beta}}. \quad \text{(C13)}$$

We now expand the exponential in both expressions. Since both are multiplied by β, we have to keep only the zeroth and the first orders, as all other terms will go to 0 in the $\beta\to\infty$ limit. We get

$$\begin{aligned}\beta[\langle AB\rangle - \langle A\rangle\langle B\rangle] \simeq \beta A(X^*)B(X^*)\Bigg\{&\sqrt{\frac{\det\boldsymbol{H}}{\det\boldsymbol{\mathcal{C}}}} - \sqrt{\frac{\det\boldsymbol{H}}{\det\boldsymbol{\mathcal{A}}}}\sqrt{\frac{\det\boldsymbol{H}}{\det\boldsymbol{\mathcal{B}}}}\\ &+\frac{1}{2\beta}\left[\frac{1}{A(X^*)^2}\nabla A\cdot\boldsymbol{\mathcal{C}}^{-1}\nabla A + \frac{1}{B(X^*)^2}\nabla B\cdot\boldsymbol{\mathcal{C}}^{-1}\nabla B + \frac{2}{A(X^*)B(X^*)}\nabla A\cdot\boldsymbol{\mathcal{C}}^{-1}\nabla B\right]\sqrt{\frac{\det\boldsymbol{H}}{\det\boldsymbol{\mathcal{C}}}}\\ &-\frac{1}{2\beta}\left[\frac{1}{A(X^*)^2}\nabla A\cdot\boldsymbol{\mathcal{A}}^{-1}\nabla A + \frac{1}{B(X^*)^2}\nabla B\cdot\boldsymbol{\mathcal{B}}^{-1}\nabla B\right]\sqrt{\frac{\det\boldsymbol{H}}{\det\boldsymbol{\mathcal{A}}}}\sqrt{\frac{\det\boldsymbol{H}}{\det\boldsymbol{\mathcal{B}}}}\Bigg\}. \end{aligned} \quad \text{(C14)}$$

We must now take the $\beta\to\infty$ limit. The $O(\frac{1}{\beta})$ terms in parentheses are easy to handle, and one gets

$$[\nabla A\cdot\boldsymbol{H}^{-1}\cdot\nabla B], \quad \text{(C15)}$$

since

$$\lim_{\beta\to\infty}\boldsymbol{\mathcal{C}} = \boldsymbol{H}, \quad \text{(C16)}$$

$$\lim_{\beta\to\infty}\boldsymbol{\mathcal{A}} = \boldsymbol{H}, \quad \text{(C17)}$$

$$\lim_{\beta\to\infty}\boldsymbol{\mathcal{B}} = \boldsymbol{H}. \quad \text{(C18)}$$

The zeroth-order term requires more caution. At the leading order in $\frac{1}{\beta}$, one has, in general,

$$\det\left(M+\frac{1}{\beta}N\right) = \det M + \frac{1}{\beta}\det N' + O\left(\frac{1}{\beta^2}\right), \quad \text{(C19)}$$

where N' is a matrix whose first row is the first row in N and all the other rows are the other rows in M. This is due to the fact that the determinant of a matrix is a linear application in each of the matrix's rows (or columns). So one gets, for the

zeroth-order term,

$$\sqrt{\frac{\det \boldsymbol{H}}{\det \boldsymbol{\mathcal{C}}}} - \sqrt{\frac{\det \boldsymbol{H}}{\det \boldsymbol{\mathcal{A}}}}\sqrt{\frac{\det \boldsymbol{H}}{\det \boldsymbol{\mathcal{B}}}} = \sqrt{\frac{\det \boldsymbol{H}}{\det \boldsymbol{H} - \frac{1}{\beta}\det \boldsymbol{\mathcal{C}}'}} - \sqrt{\frac{\det \boldsymbol{H}}{\det \boldsymbol{H} - \frac{1}{\beta}\det \boldsymbol{\mathcal{A}}'}}\sqrt{\frac{\det \boldsymbol{H}}{\det \boldsymbol{H} - \frac{1}{\beta}\det \boldsymbol{\mathcal{B}}'}} + O\left(\frac{1}{\beta^2}\right)$$
$$= \sqrt{\frac{\det \boldsymbol{H}}{\det \boldsymbol{H} - \frac{1}{\beta}(\det \boldsymbol{\mathcal{A}}' + \det \boldsymbol{\mathcal{B}}')}} - \sqrt{\frac{\det \boldsymbol{H}}{\det \boldsymbol{H} - \frac{1}{\beta}\det \boldsymbol{\mathcal{A}}'}}\sqrt{\frac{\det \boldsymbol{H}}{\det \boldsymbol{H} - \frac{1}{\beta}\det \boldsymbol{\mathcal{B}}'}} + O\left(\frac{1}{\beta^2}\right), \tag{C20}$$

and it can now be easily proven that

$$\lim_{\beta\to\infty} \beta\left(\sqrt{\frac{\det \boldsymbol{H}}{\det \boldsymbol{H} - \frac{1}{\beta}(\det \boldsymbol{\mathcal{A}}' + \det \boldsymbol{\mathcal{B}}')}} - \sqrt{\frac{\det \boldsymbol{H}}{\det \boldsymbol{H} - \frac{1}{\beta}\det \boldsymbol{\mathcal{A}}'}}\sqrt{\frac{\det \boldsymbol{H}}{\det \boldsymbol{H} - \frac{1}{\beta}\det \boldsymbol{\mathcal{B}}'}}\right) = 0. \tag{C21}$$

So the zeroth-order term adds up to 0, and we are left with

$$\lim_{\beta\to\infty} \beta[\langle A(X)B(X)\rangle - \langle A(X)\rangle\langle B(X)\rangle] = [\nabla A \cdot \boldsymbol{H}^{-1} \cdot \nabla B]\big|_{X=X^*}, \tag{C22}$$

which is our thesis. In the case where $A(X) = B(X) = \frac{1}{V}\frac{\partial U}{\partial \gamma}$, one again gets the expression

$$\frac{1}{V^2}\boldsymbol{\Xi} \cdot \boldsymbol{H}^{-1} \cdot \boldsymbol{\Xi}, \tag{C23}$$

where $\boldsymbol{\Xi} \equiv \nabla\frac{\partial U}{\partial \gamma}$. We thus recover the known athermal expression [16,23,25] for the shear modulus,

$$\mu = \frac{1}{V}\left\langle\frac{\partial^2 U}{\partial \gamma^2}\right\rangle - \beta V[\langle\sigma^2\rangle - \langle\sigma\rangle^2] \overset{\beta\to\infty}{\longrightarrow} \mu_{\text{Born}} - \frac{\boldsymbol{\Xi} \cdot \boldsymbol{H}^{-1} \cdot \boldsymbol{\Xi}}{V}. \tag{C24}$$

This shows how, in the thermal case, the mechanism for divergence of the shear moduli as a consequence of the presence of low-lying modes in the Hessian of the potential energy (i.e., marginality in the *mechanical* sense) is now replaced by a mechanism in terms of anomalous fluctuations and, as a result of the fluctuation-dissipation theorem, anomalous nonlinear response of the system to external perturbations (i.e., marginality in the *thermodynamic* sense), as discussed in the text.

[1] J. C. Dyre, Rev. Mod. Phys. **78**, 953 (2006).
[2] A. Cavagna, Phys. Rep. **476**, 51 (2009).
[3] A. Q. Tool, J. Am. Ceram. Soc. **29**, 240 (1946).
[4] T. Castellani and A. Cavagna, J. Stat. Mech.: Theory Exp. (2005) P05012.
[5] C. Rainone, P. Urbani, H. Yoshino, and F. Zamponi, Phys. Rev. Lett. **114**, 015701 (2015).
[6] C. Rainone and P. Urbani, J. Stat. Mech. (2016) 053302.
[7] H. Ritland, J. Am. Ceram. Soc. **39**, 403 (1956).
[8] L. D. Landau and E. M. Lifshitz, *Course of Theoretical Physics, Vol 7: Theory of Elasticity* (Pergamon Press, London, 1959).
[9] H. G. E. Hentschel, S. Karmakar, E. Lerner, and I. Procaccia, Phys. Rev. E **83**, 061101 (2011).
[10] S. Hess, M. Kröger, and W. G. Hoover, Physica A: Stat. Mech. Appl. **239**, 449 (1997).
[11] J. Lutsko, J. Appl. Phys. **65**, 2991 (1989).
[12] J. P. Wittmer, H. Xu, P. Polińska, F. Weysser, and J. Baschnagel, J. Chem. Phys. **138**, 12A533 (2013).
[13] A. K. Dubey, I. Procaccia, C. A. B. Z. Shor, and M. Singh, Phys. Rev. Lett. **116**, 085502 (2016).
[14] M. Born and K. Huang, *Dynamical Theory of Crystal Lattices* (Oxford University Press, New York, 1998).
[15] W. Kob and H. C. Andersen, Phys. Rev. Lett. **73**, 1376 (1994).
[16] D. L. Malandro and D. J. Lacks, J. Chem. Phys. **110**, 4593 (1999).
[17] S. Karmakar, E. Lerner, and I. Procaccia, Phys. Rev. E **82**, 026105 (2010).
[18] M. Müller and M. Wyart, Annu. Rev. Condens. Matter Phys. **6**, 177 (2015).
[19] G. Biroli and P. Urbani, arXiv:1601.06724.
[20] E. Gardner, Nucl. Phys. B **257**, 747 (1985).
[21] P. Charbonneau, J. Kurchan, G. Parisi, P. Urbani, and F. Zamponi, Nat. Commun. **5**, 3725 (2014).
[22] R. Gutiérrez, S. Karmakar, Y. G. Pollack, and I. Procaccia, Europhys. Lett. **111**, 56009 (2015).
[23] S. Karmakar, E. Lerner, I. Procaccia, and J. Zylberg, Phys. Rev. E **82**, 031301 (2010).
[24] C. M. Bender and S. A. Orszag, *Advanced Mathematical Methods for Scientists and Engineers I* (Springer Science & Business Media, Berlin, 1999).
[25] A. Lemaître and C. Maloney, J. Stat. Phys. **123**, 415 (2006).